JOURNAL OF PHYSICAL ORGANIC CHEMISTRY, VOL. 9, 795–800 (1996)

# MECHANISM OF SOLID–SOLID RESOLUTION OF PANTOLACTONE

GERD KAUPP* AND JENS SCHMEYERS

*University of Oldenburg, Organic Chemistry I, D–26111 Oldenburg, Germany*

FUMIO TODA* AND HIDEAKI TAKUMI

*Ehime University, Department of Applied Chemistry Faculty of Engineering, Matsuyama, Ehime 790, Japan*

AND

HIDEKO KOSHIMA

*Ryukoku University, Department of Materials Chemistry, Seta, Otsu 520–21, Japan*

**The enantioselective solid–solid clathration of (*S*)-pantolactone (*1*) into (*R,R*)-*trans*-2,3-bis(diphenylhydroxymethyl)-1,4-dioxaspiro[4·4]nonane (*2*) and -[4·5]decane (*3*) was studied preparatively and mechanistically using atomic force microscopy (AFM) measurements and crystal packing data. Short-distance solid-to-solid sublimation mechanisms occur in both cases with initial formation of epitaxial floes along the *b*-axis in *2* and random craters in *3*. The bulk control in the phase rebuilding stage is understood from the particular crystal packings. Bulk control was largely lost in the phase transformation stage when passivation of the surfaces occurred in both cases. The host lattices of *2* and *3* exhibit closed molecular double layers with all hydroxyl groups inside and lacking access for intercalation of *1*. The reaction has to start at isolated surface defects. Once started, new doors for further entrance of guest molecules (*S*)-*1* are opened in the double layer. For practical use, both the crystallographic difficulties and the passivation have to be overcome. A slurry technique involving addition of stoichiometric amounts of water to the solids provided useful conditions for the preparative resolution of (*R/S*)-*1* or further racemates exhibiting passivation, whereas heating alone speeded up the resolution of 2-methylpiperazine with *2*.**

## 1. INTRODUCTION

Organic solid–solid reactions cover a wide range of reaction types already;[1] however, only the solid–solid rearrangement of benzopinacol[2] and the benzilic acid rearrangement of benzil[3] have been mechanistically studied and virtually nothing is known about different mechanisms in this solvent-free technique. Enantioselective solid–solid clathrations with chiral hosts provide rewarding resolutions of racemates without solvent and various solid–solid resolutions have been successfully performed.[1] The versatile resolution of pantolactone (**1**) [its (*R*)-enantiomer being the precursor to pantothenic acid (vitamin $B_3/B_5$) synthesis][4] using the chiral host (*R,R*)-*trans*-2,3-bis(diphenylhydroxymethyl)-1,4-dioxaspiro[4·5]decane (**3**)[5] has recently been achieved.[6] Further improvement in pantolactone resolution is gratifying, because previous diastereomeric methods are not very efficient and organic solvents should be avoided. Therefore, we undertook an atomic force microscopic (AFM) study of the solid–solid interaction of (*S*)-(−)-**1** with (*R,R*)-*trans*-2,3-bis (diphenylhydroxymethyl)-1,4-dioxaspiro[4·4]nonane (**2**) and -[4,5]decane(**3**) and interpret the experimental results in the light of the crystallographic data for neat **2** and **3**.[7]

We chose the systems **1–2** and **1–3** for the first mechanistic AFM investigation of a solid–solid clathration. The data indicate that large-scale resolution of solid volatile racemates can be achieved conveniently even in the case of surface passivation.

## RESULTS

### Preliminary examinations

The freshly distilled racemate of (*R/S*)-**1** is extremely hygroscopic and deliquescent. It takes up water from moist air and forms liquid drops within 1 min or so. Thermogravimetric measurements at 25 °C show that a 1·5% increase in weight stops sharply after 90 min (relative humidity 70%) and is followed by a weight decrease due to vaporization, reaching the original weight after 5 h and then decreasing further. Such

* Author to whom correspondence should be addressed.

CCC 0894–3230/96/120795–06


*Received 4 June 1996*
*Revised 16 July 1996*

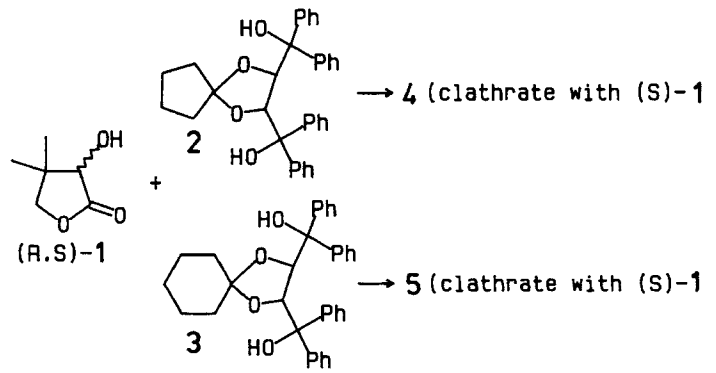


behavior is unsuitable for AFM investigations under ambient conditions. It is therefore of particular interest that the crystals of the pure enantiomers of **1** are non-deliquescent. Their rate of sublimation at 25 °C is significant: a 14% weight loss of (*S*)-**1** was detected in 5 h under ambient conditions. Polycrystalline samples (0·15 mg) of (*S*)-**1** were completely evaporated in 3 days when left in ambient air.

While the reasons for the differences in the hygroscopicity of racemic and enantiomeric crystals of **1** remain to be elucidated crystallographically, the still moderate volatility of (*S*)-**1**, subject to inclusion by (*R*,*R*)-**2** or (*R*,*R*)-**3**, does not prevent its investigation by AFM under ambient conditions. Clearly, an answer is required to the question of whether we have a solid–solid reaction solely via a solid contact interface (as in the rearrangement of benzopinacol when catalyzed by solid *p*-toluenesulfonic acid[2]) or whether we see a short-path sublimation mechanism, i.e. a particular gas–solid clathration.[3,8] It turned out that a short-distance solid-to-solid sublimation mechanism obtains in the clathration of (*S*)-**1** with (*R*,*R*)-**2** or (*R*,*R*)-**3**.

Experimental evidence is as follows: dendritic crystals of about 0·15 mg weight of (*S*)-**1** do not readily contact the (001) or (010) faces of single crystals of (*R*,*R*)-**2** or (*R*,*R*)-**3** but remain loosely lying on them during the whole period of 3 days until they have completely disappeared owing to imbibition and evaporation. Even if (*S*)-**1** was pelleted using a polished piston on a hydraulic press to obtain a smoother surface, no adhering effect with single-crystal main faces of (*R*,*R*)-**2** and (*R*,*R*)-**3** could be achieved. This behavior differs from that found previously[2] (benzopinacol and *p*-TosOH), where a firm crystal-to-crystal contact ensued from solid–solid reaction on the reactive face of the single crystal. Furthermore, the zone of reaction was sharply the projection of the polycrystal (*S*)-**1** to the surfaces of (*R*,*R*)-**2** and (*R*,*R*)-**3**. Outside that range (in the absence of solvent vapors from the atmosphere), no change of the surface of the non-volatile single crystals of the hosts was detected by AFM. Thus, sidewise sublimation of (*S*)-**1** was inefficient. Only very short distance sublimation from solid (*S*)-**1** to solid (*R*,*R*)-**2** or (*R*,*R*)-**3** was effective in clathration. In the rather uniform reaction area the feature-forming phase rebuilding, already known from gas–solid imbibitions,[3,8] occurred, forming floes with (*R*,*R*)-**2** and craters with (*R*,*R*)-**3** (see Plates 1 and 2).

## AFM surface features

The short-distance imbibition of (*S*)-**1** into (*R*,*R*)-**2** on its (001) face (Plate 1) gradually forms large floes out of a moderately rough initial plane ($R_{ms}$ = 2·89 nm). The floes with heights of up to 300 nm which are formed upon imbibition run initially [Plate 1(b) and (d)] parallel to the long crystal axis. Clearly, we have guidance of the long-range molecular movements by the crystal bulk in the stage of phase rebuilding.

The stereoscopic packing diagram of (*R*,*R*)-**2** under its main face (001) (Figure 1) shows that all molecules align along the direction of the *b*-axis. In the upper layer all molecules have the same orientation, but this differs from the uniform orientation in the lower layer of molecules. Nevertheless, diagonal rows of molecules have the same direction in both layers. That direction is also retained in the adjacent double layers. No OH groups are found between the double layers. All of these layers are parallel to (001). Hence it is understandable that the phase rebuilding features do align along the *b*-axis if the molecules move above (001) after having interacted with (*S*)-**1**, which intercalates within the double layers while forming hydrogen bonds with the OH groups present. In the neat crystal the OH groups of the host molecules form one intramolecular hydrogen bond each but are too far apart for bridging the two sheets of the double layer (IR frequencies at 3398 and 3587 $cm^{-1}$). Such intercalations cannot accommodate the neat lattice of (*R*,*R*)-**2**. Rather, the distance of the layers must increase and an upward transport of the whole material ensues well along the (100) planes. Thus, the original lattice is retained as well as possible if the features grow anisotropically.

However, such directional preference is completely lost upon long-term reaction [Plate 1(c)]. The still floe-like features grew to reach 800 nm in height, leaving deep valleys but now with random orientations. Clearly, phase transformation into the lattice of the inclusion complex has occurred in the visible part of that surface. Only that final process is hardly influenced by the original lattice of the host. However, the surface of **2** is now passivated by a dense coating of crystals at that stage. A preparative solid-state inclusion could not be achieved with **1** and **2** by that mechanism but requires breaking of the passivation.

Enantiomeric recognition of (*S*)-**1** by (*R*,*R*)-**3** exhibits completely different AFM features (Plate 2). Here the surface corrugation changes, but no large elevations occur. The characteristic craters formed upon phase rebuilding are initially (30 min) sporadic (0·8 $\mu m^{-2}$), deep (average depth 26·3 nm), steep (up to 28°) and wide (350–400 nm), but become [Plate 2(b) and (d); 2 h, 2·1 $\mu m^{-2}$] more frequent, less deep (average depth 12·8 nm), less steep (around 10°) and less wide (300–350 nm). They are almost gone after 10 h and they disappear completely thereafter [Plate 2(c)]. Clearly, initial long-range molecular movement is well guided by the crystal bulk.

Upon prolonged reaction (3 days), the phase transformation (to give the lattice of the clathrate at the surface) is complete: all craters are filled and a flat, slightly corrugated surface remains. Also here, the AFM images indicate surface passivation which has to be removed in preparative runs.

The molecular interpretation of the initial phase rebuilding is provided by the stereoscopic packing diagram in Figure 2 from the crystal structural data.[7]

As in (*R*,*R*)-**2**, all molecules within a layer have the same orientation and this differs from the structure of tetraphenylethylene (producing craters upon reaction with $NO_2$),[9] where two molecular orientations occur within each plane. However, in contrast to the lattice of (*R*,*R*)-**2** under (001), the diagonal rows of molecules under (010) of (*R*,*R*)-**3** have directions different by 84° in the adjacent sheets of a double layer. The adjacent double layers are identical with the previous ones, although turned around the *b*-axis by 180°, and thus establish two further diagonal directions adding up to a total of four different molecular orientations. The two OH groups of the host molecule again form one intramolecular hydrogen bond, leaving a free OH group, but the distance between the sheets in the double layer is too large to be hydrogen bridged (IR frequencies 3342 and 3530 $cm^{-1}$). Thus, intercalation of (*S*)-**1** with the formation of hydrogen bonds and a volume

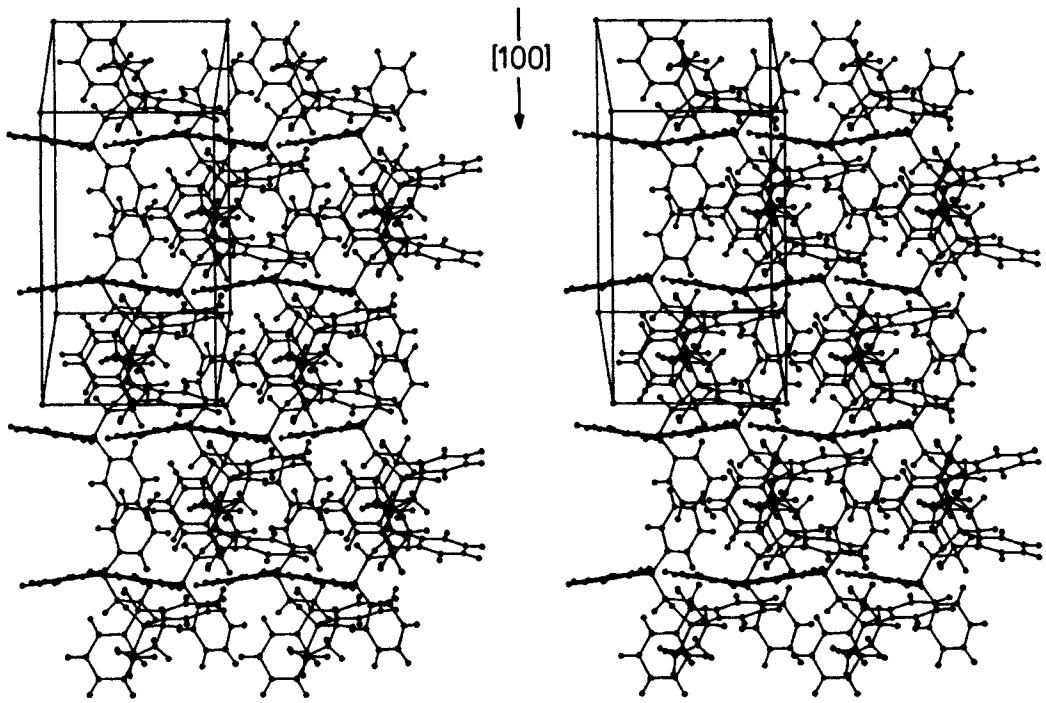


Figure 1. Stereoscopic representation of the molecular packing of (*R*,*R*)-**2** (*C*2) on (001) showing a double layer with all OH groups inside and all molecules aligned along the *b*-axis

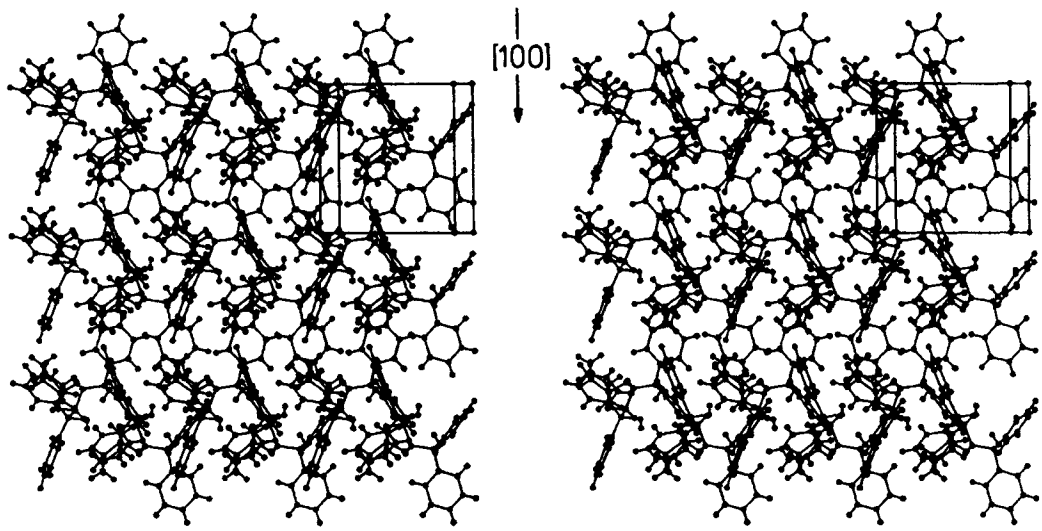


Figure 2. Stereoscopic representation of the molecular packing of (*R,R*)-**3** ($P2_12_12_1$) on (010) showing a double layer with all OH groups inside; the molecules form rows along their long axes which intersect the *c*-axis at 48 ° (upper layer) and 132 ° (lower layer)

increase cannot be answered with vertical transports parallel to a plane as in the situation of the host (*R,R*)-**2**. Rather, spiral movements up and down through several layers with tilting of the widened parts of the double layers are indicated. Such movements form the craters which are observed in Plate 2. The low density of the host crystals (*R,R*)-**3** indicate a loose packing and indeed some voids are recognizable if the crystal packing is viewed under (001) (not imaged here). Hence, there is ample space available for turns and tilts to build the craters.

Based on the densities of relaxed crystals [(*R,R*)-**3**, $D = 1{\cdot}208$ g cm$^{-3}$;[7] **5**, $D = 1{\cdot}229$ g cm$^{-3}$],[6] there must be an overall volume increase by about 24% (the mass increase is 26%). Nevertheless, the molecular movements produce craters although apparently with transport of material above the original (010) surface in the stage of phase rebuilding. Overall volume increases cannot be depicted in planefit-based AFM images as in Plate 2(b) and (d). However, it is true that the initial craters fill up upon continuation of the reaction [Plate 2(c)]. It is to be concluded that the surface level at the later stage in Plate 2(c) is actually higher than that in Plate 2(a) with respect to the crystal base. Clearly, only the processes that are observed in the initial stages of the imbibitions are strictly governed by the crystal bulk.

## DISCUSSION

The detailed observations of the submicroscopic events with the AFM show again that phase rebuilding occurs with long-range anisotropic molecular movements, followed by phase transformation into the product lattice.[10] Therefore, in these non-topotactic supramolecular reactions no interpretational basis exists for smoothly transforming the starting lattice into the final lattice, say with relation to fixed reference coordinates. Rather, chemical reactivity depends on the possibility for long-range molecular movements along 'easy ways' that can be derived from and related to the crystal lattice for the initial stage of the reaction. Thus, the completely different mechanisms for clathration of solid hosts (*R,R*)-**2** and (*R,R*)-**3** (both under their most prominent face, prior to the passivation) are understood from their molecular packings.[10] The mechanistic data clearly indicate short-distance crystal-to-crystal sublimation.

An important question is the mechanism of intercalation into the closed double layers which run parallel to the investigated crystal faces in both hosts studied. There are no 'open doors' large enough for (*S*)-**1** to enter, nor can single host molecules be pushed away (see Figures 1 and 2). The initially sporadic formation of craters in the imbibition of (*R,R*)-**3** is a clear indication that the reaction starts at isolated defect points on the surface. Molecular packing defects may be present at dislocations or they may have been created by manipulating the crystal. Once started, the phase rebuilding with long-range movements opens the doors for further entry of guest molecules of suitable chirality[6] in both cases, but this has to be done over and over again for every double layer, the rebuilt lattice trying to accommodate the chemically changed

situation. At the rare points of contact of the tiny laid-on polycrystal a similar situation obtains once the mechanical defects have been used for initial clathration. Thus, such isolated points could not be found on the developing reactions over the surface of the single crystals of **2** and **3**.

The mechanistic data show that the start and the continuation of the intercalation process are difficult both for crystallographic reasons and because of passivation. Hence for practical use it appears important to increase the rate of reaction and break the passivation. One way to do this is to increase the temperature and, indeed, we succeeded in complete inclusion of (*S*)-**1** into **3** at 80 °C, still below the desorption temperature. Unfortunately, the racemic crystals of (*R*/*S*)-**1** are liquid at that temperature and no useful rates could be obtained. As passivation cannot be overcome by pelleting powders of (*R*/*S*)-**1** and **3**, it was necessary to use the solubility of the former in water for a preparative slurry technique. The concentrated solution transports (*S*)-**1** efficiently to the surface of **3** for inclusion at room temperature and the water breaks the passivating layer on **3** [Plate 2(c)]. Hence larger scale runs succeed within 1 week at room temperature.

The present results add a new mechanism to the series of solid–solid reactions. This mechanism may be general for all kinds of volatile solids and its application to the technical resolution of further volatile racemates will be rewarding if passivation to the surface does not occur. A typical example is the optical resolution of *rac*-2-methylpiperazine with **2** (2 : 1 inclusion complex, 87% *ee*, 5 days at room temperature or 5 h at 80 °C; apparently no passivation here).[11] If, however, passivation occurs, the slurry technique by addition of 2 equivalents of water may be helpful. Thus, the optical resolution of *rac*-α-amino-ε-caprolactam by **2** requires the slurry technique (99% *ee*, 5 days at room temperature).[11]

## EXPERIMENTAL

Single crystals of neat (*R*,*R*)-(−)-**2** were obtained as plates from diethyl ether–hexane (1 : 1 v/v). Flat prisms of (*R*,*R*)-(−)-**3** were obtained from toluene–hexane (1 : 1 v/v). Freshly sublimed (*S*)-**1** formed dendritic polycrystals. They were used directly as 0·15 mg samples or as small parts of pellets which were pressed by using a polished steel piston ($R_{ms}$ = 100 nm) of an IR-equipment hydraulic press. Samples of (*S*)-**1** were laid down on the single crystals of (*R*,*R*)-**2** and (*R*,*R*)-**3** for the times given. For AFM measurements with a Nanoscope II and the imaging of packing diagrams with Schakal, see Refs. 8, 9 and 12. Thermogravimetric measurements were made using a Perkin-Elmer TGA-7 instrument.[8]

The structural crystal data will be published elsewhere:[7] (*R*,*R*)-**2** (*C*2), $a$ = 15·700, $b$ = 9·325, $c$ = 18·4551 Å, $\beta$ = 105·372°, $D$ = 1·256 g cm$^{-3}$; (*R*,*R*)-**3** ($P2_12_12_1$), $a$ = 10·212, $b$ = 29·284, $c$ = 9·314 Å, $D$ = 1·208 g cm$^{-3}$; **5** [1 : 1 clathrate of (*S*)-**1** in (*R*,*R*)-**3**] ($P2_1$), $a$ = 10·563, $b$ = 9·692, $c$ = 17·008 Å, $\beta$ = 98·86°, $D$ = 1·229 g cm$^{-3}$.[6]

*Solvent-free inclusion of (S)-1 into 3.* A 1·00 g (7·7 mmol) amount of solid (*S*)-**1** (m.p. 96 °C) was mixed with 3·91 g (7·7 mmol) of **3** and kept in a closed vessel under 1 bar of dry air at 80 °C for 6 h. All (*S*)-**1** was included and the 1 : 1 clathrate was formed quantitatively [4.91 g (100%)]. The IR spectrum corresponded to that found from crystallization[6] with the sharp OH band of the free host at 3342 cm$^{-1}$ missing. TGA released the guest **1** at 138 °C (20 °C min$^{-1}$; inflection point) starting at about 100 °C, with a total weight loss of 22·3%.

(*R*/*S*)-**1** (m.p. 74–78 °C) was liquid at 80 °C, which is unfavorable for solid-state reactivity. Vapors of the guest from (*R*/*S*)-**1** were only slowly taken up by **3** at 80 °C (in dry air, 2·5% in 6 h).

*Preparative slurry resolution of (R/S)-1.* A mixture of 1·00 g (1·98 mmol) of **3**, 0·52 g (4·0 mmol) of (*R*/*S*)-**1** and 0·14 g (7·8 mmol) of water formed a stiff slurry when ground in a mortar. It was kept for 5 days at room temperature, washed with 50 ml of water with suction to remove uncomplexed (*R*)-**1** and dried, leaving 1·21 g of the inclusion complex as a colorless powder which liberated 0·21 g (80%) of (*S*)-**1** with 82% *ee* {[α]$_D$ −39·5° (*c* 1·33, $H_2O$)}. The optical purity was determined by HPLC using the chiral phase Chiralcel OA.

The 1 : 1 inclusion complex **5** starts to liquefy at 150 °C and completely melts at 184 °C; IR (KBr), 3343 (very broad, OH), 1767 (C=O) cm$^{-1}$. $^1$H NMR ($CDCl_3$), δ = 7·54–7·21 (20 H, arom.), 4·552 (s, 2 H, CH of **3**), 4·10–3·93 (0·8×3 H, $CH_2$ and CH of **1**), 2·56 (br s, 2 H, OH of **3**), 1·40–1·14 (10 ring H of **3**), 1·236 (s, 0·8×3 H, $CH_3$ of **1**), 1·080 (s, 0·8×3 H, $CH_3$ of **1**). The recrystallized 1 : 1 inclusion complex **5** was analysed by combustion: calculated for $C_{40}H_{44}O_7$, C 75·45, H 6·96; found, C 75·39, H 7·20%. If the filtrate was evaporated and the residue sublimed at 2 Torr, 0·31 g (120%) of (*R*)-**1** {*ee* 56%, [α]$_D$ + 27·9° (c 0·50, $H_2O$)} were obtained.

The solubilities of **2** and **3** in water were 0·32 and 0·61 g l$^{-1}$, respectively.

## REFERENCES

1. F. Toda, in *Reactivity in Molecular Crystals*, edited by Y. Ohashi, pp. 177–201, Kodansha, Tokyo, and VCH, Weinheim (1993); *Acc. Chem. Res.* **28**, 480–486 (1995).
2. G. Kaupp, M. Haak and F. Toda, *J. Phys. Org. Chem.* **8**, 545–551 (1995).

3. G. Kaupp, J. Schmeyers, M. Haak, T. Marquardt and A. Herrmann, *Mol. Cryst. Liq. Cryst.* **276**, 315–337 (1996).
4. E. T. Stiller, S. A. Harris, J. Finkelstein, J. C. Keresztesy and K. Folkers, *J. Am. Chem. Soc.* **62**, 1785–1790 (1940); C. Hatat, A. Karim, N. Kokel, A. Mortreux and F. Petit, *Tetrahedron Lett.* **29**, 3675–3678 (1988), and references cited therein.
5. D. Seebach, A. K. Beck, R. Imwinkelried, S. Roggo and A. Wonnacott, *Helv. Chim. Acta* **70**, 954–974 (1987).
6. F. Toda, A. Sato, K. Tanaka and T. C. W. Mak, *Chem. Lett.* 873–876 (1989).
7. F. Toda, K. Tanaka, H. Miyamoto, H. Koshima, I. Miyahara and K. Hirotsu, *J. Chem. Soc. Perkin Trans. 2.* submitted for publication.
8. G. Kaupp, U. Pogodda and J. Schmeyers, *Chem. Ber.* **127**, 2249–2261 (1994).
9. G. Kaupp and J. Schmeyers, *J. Org. Chem.* **60**, 5494–5503 (1995).
10. G. Kaupp, Adv. *Photochem.* **19**, 119–177 (1995); in *Comprehensive Supramolecular Chemistry*, edited by J. E. D. Davies, Vol. 8., pp. 381–423, Elsevier, Oxford (1996), and references cited therein.
11. F. Toda and H. Takumi, *Eucentiovrer* **1**, 29–33 (1996).
12. G. Kaupp, *GIT Fachz. Labor* **37**, 284–294, 581–586 (1993); G. Kaupp, J. Schmeyers, M. Haak and A. Herrmann, *Labo-Trend* **26**(6), 57–63 (1995); English translations of these reviews are available in WWW under *http://kaupp.chemie.uni-oldenburg.de.*